Section 3. Ceramics

Vibrational investigation of sintered titanium biomaterials

V. SIMON[*], C. POPA[a], D. MURESAN, S. SIMON

Babes-Bolyai University, Faculty of Physics, Cluj-Napoca 400084, Romania
[a]Technical University of Cluj-Napoca, Faculty of Materials Science and Engineering, Cluj-Napoca 400020, Romania

Titanium-hydroxyapatite (Ti-HA) composites were obtained by sintering 95 wt% titanium and 5 wt% hydroxyapatite type calcium phosphates powder prepared by sol-gel method. X-ray diffraction (XRD) and infrared analysis confirm the development of HA type crystallites in the sol-gel samples. Ti and HA powders were pressed without the use of any lubricant. The bioactivity of composite Ti-HA was tested in simulatated body fluid. Biologically active hydroxyapatite similar to the mineralised bone tissue was developed *in vitro* under *in vivo* simulated conditions. Raman spectroscopy and XRD data evidence the development on composite surface of hydroxyapatite type phase after (simulated body fluid) soaking.

1. Introduction

Local defects in bone as a result of disease or trauma are frequently restored by bone graft substitutes. Calcium phosphate ceramics, especially hydroxyapatite and β-tricalcium phosphate are widely used for hard tissue replacement due to their biocompatibility and osteoconductive properties [1,2]. These ceramics are utilized in powder and block forms as bone defect fillers. Hydroxyapatite, HA $(Ca_{10}(PO_4)_6(OH)_2)$, is an important biomaterial, and is the principal inorganic constituent of bones and teeth. In situ mineralization of HA and the role of organics in initial nucleation and growth of HA is critical for the resulting nano and microstructure of HA. Biologically active hydroxyapatite similar to the mineralised bone tissue may be developed *in vitro* under *in vivo* simulated conditions. Hydroxyapatite is both biocompatible and bioactive, but its poor mechanical properties, such as low strength and limited fatigue resistance, limit the pure hydroxyapatite applications in load bearing implants.

Among metallic implant materials titanium is largely used because it is highly biocompatible and its density is considerably lower than that of stainless steels [3]. In order to improve the bone attachment, bioactive hydroxyapatite layer deposition is often used for "biomimetic"coating [4] of titanium implants. Titanium-hydroxyapatite (Ti-HA) composites are extensively studied as potential bone replacement materials. New functionally graded materials based on sintered titanium and hydroxyapatite powders are much adequate as bone substitute because they have bioactive properties and provide enhancement in mechanical properties [5-7].

This study presents the results of infrared spectroscopic analysis of hydoxyapatite type powders obtained by sol-gel method and of Raman investigation of the graded layer formed after immersion of sintered Ti-HA powders in simulated body fluid.

2. Experimental

High purity titanium powder (grain size between 63 and 100 μm) and hydroxyapatite powder (grain size less than 40 μm) were used for sintering Ti-HA composite samples. Hydroxyapatite was prepared by sol-gel method. The precursor reagents were $Ca(NO_3)_2$ and $(NH_4)_2HPO_4$. The Ca/P molar ratio in precursors was 1.67 because like in the major mineral phase of the bone $Ca_{10}(PO_4)_6(OH)_2$ (hydroxyapatite). The dried sol-gels were heat treated in air for 3 hours at 900°C and for 1 hour at 1150 °C. Titanium powder with 5 wt % HA (95Ti-5HA) was mixed in a tubular mixer. Powders were pressed by applying forces of 30 and 35 kN in a rigid die with the surface of 0.5 cm^2, without the use of any lubricant. The compacts were subsequently vacuum sintered (10^{-6} torr) at 1160 °C for 60 minutes, with dwelling stages at 200, 600 and 800 °C.

Bioactivity was investigated by an in-vitro test. The samples were soaked in simulated body fluid (SBF) solution [8]. SBF volume to sample surface was around 30 m, according to the soaking conditions in such experiments. For structural characterization of the HA sol-gel samples X-ray diffraction (XRD) and Fourier transform infrared (FTIR) attenuated total reflectance (ATR) microspectroscopy were used. For estimating the response to SBF exposure the samples were analysed by XRD and Raman spectroscopy. X-ray diffraction, FTIR

and Raman analyses were carried out on Bruker equipments at room temperature.

3. Results and discussion

The X-ray diffraction pattern of as prepared sol-gel sample (Fig. 1a) reveals features of hydroxyapatite type crystallites. The principal diffraction peaks of HA [9] appears at 2θ values of 25.9° for reflection (002), at 31.9° (triplet) for reflections (211), (112) and (300), and at 34.0° for reflection (200). The crystal size D was estimated from diffractograms using the Scherrer formula [10]

$$D = \frac{k \cdot \lambda}{\beta_{1/2} \cdot \cos \theta} \qquad (1)$$

where D is the size in Å, k is a shape factor equal to 0.9, λ is the wavelength of X-rays, θ is the diffraction and $\beta_{1/2}$, expressed in radians, is defined as $\beta_{1/2} = \sqrt{B^2 - b^2}$ where B is the diffraction peak width at half height and b is the natural width of the instrument. Using the corresponding data for the (002) reflection a mean size of 8.2 nm is obtained.
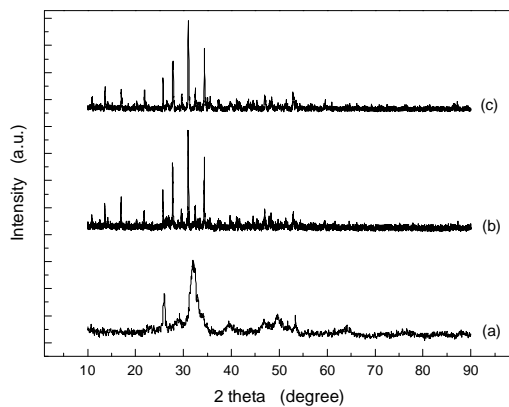

Fig. 1. XRD patterns of the (a) as prepared, (b) heat treated at 900 °C and (c) heat treated at 1150 °C sol-gel HA type sample.

After heat treatments at 900 and 1150 °C well defined crystalline phases of hydroxyapatite type (Fig. 1b and c), with crystals much larger than in as prepared sol-gel HA sample, are developed. The examination of the influence of heat treatment temperature on as prepared HA sol-gel powder shows that the structure of the developed crystalline phases are stable up to 1150 °C.

The same conclusion is mainly supported by the feature stability of the absorption bands from IR spectra of the samples heat treated at 900 and 1150 °C (Fig. 2). The IR characteristic peaks of phosphate groups in HA appear between 1030-1090, 900-950 and 560-600 cm^{-1} [11,12]. Similar IR bands for the phosphate units were recorded from a sol–gel derived bioactive glass–ceramic [13]. The bands recorded around 680, 760, and 1250 cm^{-1} from the

sample heat treated at 900 °C (Fig. 2a) are not evidenced for the sample heat treated at 1150 °C (Fig. 2b). One observes that instead of the well developed bands occurring at 790 and 1310 cm^{-1} in the spectrum of the sample heat treated at 900 °C, very large bands appear for the sample heat treated at 1150 °C. These bands occur in the IR spectrum of β-tricalcium-phosphate crystals [12], that is also a crystalline component entering in the mineral phase of bone tissue.

Since no differences are seen in the XRD pattern regarding the crystallinity the samples heat treated at 900 and 1150 °C, these changes in the FTIR spectra are indicative of small rearrangements in the local environment and bonding in HA type sol-gel samples heat treated at these temperatures. Particularly the large IR bands recorded around 790 and 1310 cm^{-1} for the sample heat treated at 1150 °C show that a vitrification process is starting at this temperature.
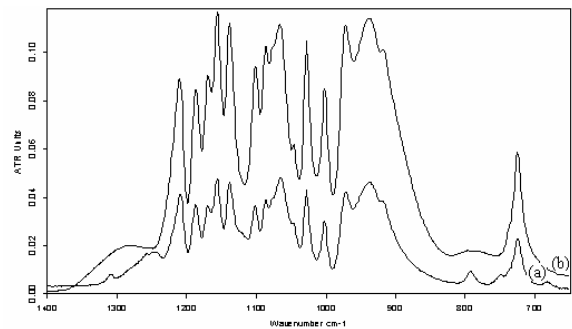

Fig. 2. FTIR ATR spectra for HA sol-gel sample heat treated at 900 °C for 3 hours (a) and at 1150 °C for 1 hour (b).
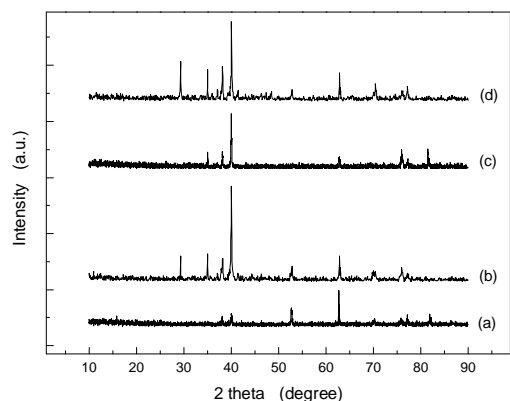

Fig. 3. XRD patterns of samples pressed under 30 kN (a, b) and 35 kN (c, d), before (a, c) and after (b, d) soaking in SBF.

After sintering 95Ti-5HA composite samples, like in the case of 90Ti-10HA [14], only a-titanium metallic phase is identified [15] in the XRD patterns of the obtained samples (Fig. 3 a and c).

The absence of any lines associated with hydroxyapatite type phases points out that after sintering process these phases are very distorded or/and partially

vitrified. The titanium metallic phase seems to consists in crystals preferentially oriented to the sample surface, depending on the sintering preasure. HA type polycrystalline phases developed at the surface of Ti-HA powder sintered samples after seven days immersion in SBF confirmed in XRD pattern (Fig. 3b and d) by appearance of new intense lines at $2\theta = 29.5^{o}$ and 35°. An other effect of the SBF soaking is observed on the titanium microcrystals orientation on the sample surface, that are after seven days immersion in SBF randomly oriented.

The Ti-HA sintered sample is Raman silent before immersion in SBF, i.e. it does not reveal any spectroscopic feature (Fig. 4a and c). After 7 days immersion in simulated body fluid the Raman spectra (Fig. 4b and d) evidence changes on the surface layer of Ti-HA sample. The line at 1083 cm^{-1} occurs from calcium hydroxyapatite [16] developed by surface mineralisation in SBF.
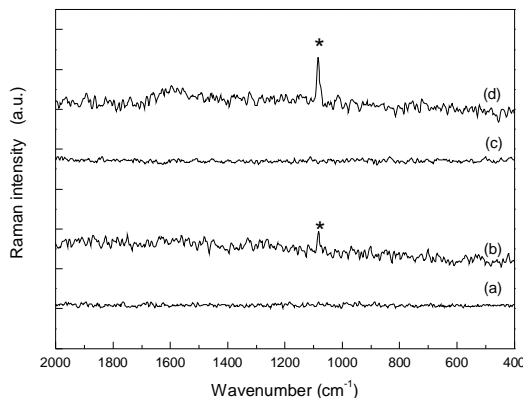

Fig. 4. Raman spectra for Ti-HA sintered sample (a) before and (b) after seven days soaking in SBF.

The Raman band recorded at 1040–1045 cm^{-1} from a human bone ex vivo formed is assigned to P–O stretches [17]. In our samples the band position is expected to vary because the local ion environments of the phosphate mineral lattice.

4. Conclusions

The sintered Ti-HA samples incorporating 5 wt % HA type phase prepared by sol-gel develop on sample surface in simulated body fluid a bioactive layer. The as prepared sol-gel HA phase contains nanocrystals sized under 10 nm, while in crystalline hydroxyapatite type powders used for sintering Ti-HA composites the crystals are much larger. The IR analysis of the heat treated HA phase evidence beside bands characteristic to hydroxyapatite also absorption bands arising from β-tricalcium-phosphate. Both crystalline phases enter in the mineral composition of bone tissue. The Raman results prove the growth of an bioactive layer on the Ti-HA sample after immersion in simulated body fluid.

References

[1] R. Z. LeGeros, Clin. Mater. **14**, 65 (1993).
[2] L. L. Hench, J. Wilson, eds., An Introduction to Bioceramics, vol. I, World Scientific, Singapore 1993.
[3] S. G. Steinemann, Injury **27**, 3, S-C16 (1996).
[4] F. Barrere, P. Layrolle, C. A. van Blitterswijk, K. De Groot, Bioceramics **12**, 125 (1999).
[5] T. Miyazaki, H. M. Kim, F. Miyaji, T. Kokubo, T. Nakamura, Bioceramics **10**, Elsevier Science LTD, 1997.
[6] H. M. Kim, F. Miyaji, T. Kokubo, T. Nakamura, J. Ceram. Soc. Jpn. **105**, 2, 111 (1997).
[7] D. A. Cortes, J. C. Escobedo, A. Nogiwa, A. Munoz: Mater. Sci. Forum **442**, 61 (2003).
[8] T. Kokubo, S. Ito, Z. T. Huang. T. Hayashi, S. Sakka, T. Kitsugi, T. Yamamuro, J. Biomed. Mater. Res. **24**, 331 (1990).
[9] R. Z. Legeros, in: Calcium Phosphates in Oral Biology and Medicine, vol. 15 in Monographs in Oral Science, Ed. H.M. Myers, Karger, Basel 1991, p. 4.
[10] H. P. Klug, L. E. Alexander, X-ray Diffraction Procedures. John Wiley, New York 1954.
[11] K. Katti, P. Gujjula, 15th ASCE Engineering Mechanics Conference, June 2-5, 2002, Columbia University, New York.
[12] J. Torrent-Burgues, R. Rodriguez-Clemente, Cryst. Res. Technol. **36**, 8-10, 1075 (2001).
[13] S. Abiraman, H. K. Varma, T. V. Kumari, P. R. Umashankar, A. John, Bull. Mater. Sci. **25**(5), 419 (2002).
[14] V. Simon, D. Muresan, C. Popa, S. Simon, The 8-th Romanian Biophysics Conference, Advanced Biomaterials and Biophysical Techniques, Iasi, May 26-28, 2005, p. 63.
[15] R. Sailer, G. McCarthy, JCPDS 44-1294, Int. Centre for Diffraction Data, 1993.
[16] J. F. Shackelford: Mater. Sci. Forum **293**, 99 (1999).
[17] S. Kale, S. Biermann, C. Edwards, C. Tarnowski, M. Morris, M. W. Long, Nature Biotechnol. **18**, 654 (2000).

*Corresponding author: simons@phys.ubbcluj.ro